Solution NMR Studies of Antiamoebin, a Membrane Channel-Forming Polypeptide

T. P. Galbraith,* R. Harris,[†‡] P. C. Driscoll,[‡§] and B. A. Wallace*

*School of Crystallography, Birkbeck College, University of London, London WC1E 7HX, UK; [†]Bloomsbury Centre for Structural Biology, Birkbeck College and University College, University of London, London WC1E, UK; [‡]Department of Biochemistry and Molecular Biology, University College, University of London, London WC1E 6BT, UK; and [§]Ludwig Institute of Cancer Research, UCL School of Medicine Branch, London W1P 8BT, UK

ABSTRACT Antiamoebin I is a membrane-active peptaibol produced by fungi of the species *Emericellopsis* which is capable of forming ion channels in membranes. Previous structure determinations by x-ray crystallography have shown the molecule is mostly helical, with a deep bend in the center of the polypeptide, and that the backbone structure is independent of the solvent used for crystallization. In this study, the solution structure of antiamoebin was determined by NMR spectroscopy in methanol, a solvent from which one of the crystal structures was determined. The ensemble of structures produced exhibit a right-handed helical C terminus and a left-handed helical conformation toward the N-terminus, in contrast to the completely right-handed helices found in the crystal structures. The NMR results also suggest that a ''hinge'' region exists, which gives flexibility to the polypeptide in the central region, and which could have functional implications for the membrane insertion process. A model for the membrane insertion and assembly process is proposed based on the antiamoebin solution and crystal structures, and is contrasted with the assembly and insertion mechanism proposed for other ion channel-forming polypeptides.

INTRODUCTION

The antiamoebins are a family of peptides produced by fungi of the species *Emericellopsis* that have antibiotic properties against the organism responsible for amoebic dysentery (Thirumalachur, 1968). Up to 16 microheterogeneous members of the family have been identified, termed antiamoebin I, II, etc., (Pandey et al., 1977; Pandey et al., 1978; Jaworski and Brukner, 2000). Antiamoebin I has the primary structure:

$$\begin{aligned} &\text{Ac}^{1}\text{-Phe}^{2}\text{-Aib}^{3}\text{-Aib}^{4}\text{-Aib}^{5}\text{-Iva}^{6}\text{-Gly}^{7}\\ &\text{-Leu}^{8}\text{-Aib}^{9}\text{-Aib}^{10}\text{-Hyp}^{11}\text{-Gln}^{12}\\ &\text{-Iva}^{13}\text{-Hyp}^{14}\text{-Aib}^{15}\text{-Pro}^{16}\text{-Phl}^{17}, \end{aligned}$$

where Ac is an acetyl group, Aib is α-aminoisobutyric acid (α-methylalanine), Iva is D-isovaline (α-ethylalanine), Hyp is hydroxyproline, and Phl is phenylalaninol.

The peptaibols, including antiamoebin, are considered good models for studying ion channels, as they form stable, well characterized channels and are relatively abundant (Wallace, 2000). They also fall in the intermediate size range where both NMR spectroscopic and x-ray crystallographic techniques can be used to investigate three-dimensional structure.

High-resolution crystal structures of antiamoebin I published by Snook et al. (1998) and Karle et al. (1998) in different environments (methanol and octanol, respectively) and in different crystallographic space groups, show that the molecule has essentially the same backbone conformation in both environments. The polypeptide backbone atoms of the two crystal structures have a positional root mean square deviation (RMSD) of 0.24 Å (Wallace et al., 2000). The structures are mostly helical, with an N-terminal α-helix (residues 1-9) followed by a small segment of 3_{10}-helix (residues 10-12) joined to an overlapping series of β-turns at the C-terminus (residues 12-16), which is sometimes described as a β-bend-ribbon (Di Blasio et al., 1992). The molecule has a deep bend centered on residue Hyp^{11}, forming an angle of 56° between the two helix axes in the methanol crystal form (Snook et al., 1998).

The molecular conformations of other naturally occurring peptaibols determined by x-ray crystallography (Fox and Richards, 1982; Karle et al., 1991; Toniolo et al., 1994; Karle et al., 1998) or NMR spectroscopy (Esposito et al., 1987; Franklin et al., 1994; Anders et al., 2000; Balashova et al., 2000; Shenkarev et al., 2002) are predominantly helical, although they differ considerably in some parameters, such as bend-angle and helical type (3_{10} versus α-helical). A regularly updated database of peptaibol sequences, along with a collection of atomic coordinates, can be found at http://www.cryst.bbk.ac.uk/peptaibol (Chugh and Wallace, 2001). The peptaibols, which now number more than 200, have been grouped into nine different subfamilies (SFs) based on their structure and function (Chugh and Wallace, 2001). These have high sequence homology and are essentially groupings of naturally occurring ''mutants.'' Comparative studies between the SFs demonstrate that quite subtle differences in sequence can lead to substantial variations in activity, and thus these molecules are a valuable resource for investigating structure/function properties. Antiamoebin is the only member of SF2 whose structure has been determined.

Submitted June 17, 2002, and accepted for publication August 05, 2002.

R. Harris's present address is The Burnham Institute, 10901 N. Torrey Pines Rd., La Jolla, CA 92037 USA.

Address reprint requests to B. A. Wallace. Tel.: (+44) 20 7631 6857; Fax: (+44) 20 7631 6803; E-mail: b.wallace@mail.cryst.bbk.ac.uk.

0006-3495/03/01/185/10 $2.00

This study aimed to determine the detailed three-dimensional structure of antiamoebin I in methanol using NMR spectroscopy, thereby allowing direct comparison between solution and solid-state structures for this molecule. This study is unique in that it is the first time one of the peptaibol structures has been determined both in solution and in the solid state in the same solvent. Comparisons of the NMR and crystal structures thus provide information on environmental effects (i.e., isotropic versus anisotropic, solution versus crystal) and on peptide flexibility, that may be relevant to membrane insertion and function of this ion-channel forming polypeptide.

EXPERIMENTAL

Antiamoebin I (Sigma, St. Louis, MO), was dissolved in either methanol-d4 (CD_3OD; Aldrich, Gillingham, UK), or methanol-d3 (CD_3OH; Aldrich), to a concentration of ~5 mg/ml (CD_3OD) or ~15 mg/ml (CD_3OH).

Data collection

NMR experiments were performed on a 500-MHz Varian Unity+ spectrometer. All two-dimensional data (except the magnitude mode COSY) were recorded in phase sensitive mode using the States-TPPI method for quadrature detection (Marion et al., 1989), and data were apodized with shifted cosine-bell squared functions, followed by zero filling once in each dimension. Water suppression in all homonuclear experiments was achieved using WATERGATE (Sklenar et al., 1993). COSY, TOCSY, one-dimensional ^{1}H, E.COSY, ROESY, NOESY and (^{1}H-^{13}C)-HSQC experiments were recorded on the methanol-d4 sample, at 298 K.

One-dimensional ^{1}H, TOCSY, ROESY, NOESY, (^{1}H-^{15}N)-HSQC and (^{1}H-^{13}C)-HMBC experiments were recorded on the methanol-d3 sample. ^3J(HN-Hα) values were obtained from the ^{1}H spectrum, whereas ^3J(Hα-Hβ) coupling constants were measured from the E.COSY spectra. All methanol-d3 spectra were acquired at a temperature of 293 K, except the NOESY experiments, which were recorded at 278 K. A set of one-dimensional spectra were recorded at temperatures between 279.5 K and 313 K, in 5 K steps, to determine the temperature dependence of the chemical shifts of the amide protons.

Spectral assignment

Assignments of the resonances to specific protons of antiamoebin were carried out using information from the COSY, TOCSY, HMBC, and HSQC spectra, based on established techniques (Wüthrich, 1986). These assignments were then used to analyze the Overhauser effect data acquired in the ROESY and NOESY experiments.

Identification of the methyl resonances for the Aib and Iva residues was the most difficult part of the assignment process, because of the number of overlapping peaks involved. To carry out the assignment, we used amide resonance information from the (^{1}H-^{15}N)-HSQC, and linked them with carbon and proton resonances from the (^{1}H-^{13}C)-HMBC and TOCSY spectra. By a process of elimination and ''walking'' along the connectivities in the residues, we assigned all the methyl peaks to specific residues. Due to the primary structure, it was not possible to assign all of the resonance peaks to their atoms stereospecifically, leading to the need for pseudoatom terms in the structure modeling process.

Distance restraints

Initial distance restraints were derived from the ROESY spectra, by the r^{-6} method (Wüthrich, 1986; Hoogstraten and Markley, 1996; Gratias et al., 1998) using integrated resonance peak volumes. Ninety upper bound distance restraints were derived from crosspeaks in the 150-ms mixing time experiment, with only 69 of the corresponding crosspeaks seen in the 500-ms experiment. The distances were entered into a simulated annealing refinement protocol using the X-PLOR program (Brünger, 1992). During the course of the structural calculations, it became clear that the number and accuracy of these semiquantitative distance restraints alone was insufficient to produce a consistent structural ensemble.

The MARDIGRAS/CORMA package (Borgias and James, 1989; 1990) was then used to calculate proton-proton distances and error bounds from the crosspeak intensities in the NOESY and ROESY spectra. The MARDIGRAS output distances were averaged for all the Overhauser effect data (3 NOESY and 2 ROESY mixing times) and used as distance restraints for simulated annealing refinement using the X-PLOR program. Each experiment was scaled in proportion to the average crosspeak intensity of the β-methylene protons, with a corresponding distance of 1.8 Å. Error bounds were added, using values of $\pm$ 1 standard deviation unit from the averaging process. Approximately 30 of the measured intensities were found in only one experiment, and therefore did not have a standard deviation from averaging. For these data we added $\pm$20% of the calculated distance as error bounds. The total number of distance restraints derived from the MARDIGRAS program was 120.

Distance restraints that were impossible to assign stereospecifically (90 out of the total 120) were entered using pseudoatom terms during initial structure determination. They were resolved in an iterative manner by measuring the specified distances in the resultant model structures and assigning the pseudoatoms accordingly. Eventually a set of 87 restraints was obtained which combined the two sets of restraints (from the r^{-6} method and the MARDIGRAS output) and produced few or no restraint violations during

simulated annealing. Of these 87 restraints, 60 specified pseudoatom terms resolved in the manner described above.

The primary structure of antiamoebin led to a lack of suitable coupling constant data from which to derive torsion angle restraints, and those which were measured were not of sufficient precision to be utilized. Therefore, no dihedral angle restraints were applied in the structure determination.

Simulated annealing refinement

One hundred random-configuration starting conformers were created and subjected to a simulated annealing run of the X-PLOR program. The 20 lowest energy conformers from each run were selected, and aligned to the lowest energy conformer using the LSQKAB program (CCP4 suite of programs: Bailey, 1994).

Analysis of preliminary structures

Hydrogen bonding in the preliminary ensembles was detected using two programs: SYBYL (Tripos Assoc., Inc., St. Louis, USA; Vanopdenbosch et al., 1985) and HBPLUS (McDonald and Thornton, 1994). Hydrogen bonding associations detected in at least 15 of the 20 lowest energy conformers by both programs were specified as distance restraints for subsequent runs of the simulated annealing protocol, similar to the method described by Balashova et al., (2000). Seven hydrogen bonds were assigned, with two standard distance restraints (O—N and O—HN) for each one. The resulting ensembles retained all the constrained hydrogen bonds after each simulated annealing run.

Temperature coefficient analysis of the relevant amide proton resonance peaks was carried out, following the change in chemical shift over a range of temperatures (from 279.5 to 313 K, in 5 K steps). The lower temperature dependence coefficients supported the involvement of the residues previously identified by SYBYL and HBPLUS in hydrogen bonding, as shown in Fig. 5, but were not used as criteria for assignment of the hydrogen bonds in the refinement procedure. It should be noted that the assignment of the acceptor groups for the suggested hydrogen bonds cannot be confirmed by experimental data without ^{13}C, ^{15}N-isotope labeling of the polypeptide. Therefore the assignments of the acceptor groups are based solely on the distance- and angle-based analyses of SYBYL and HBPLUS.

Monitoring of the model structures used as templates for subsequent runs of simulated annealing was carried out with PROCHECK (Laskowski et al., 1993), and only those which had no residues in the disallowed regions of the Ramachandran plot were used further.

The SYBYL program was used to display the molecules shown in Figs. 3 and 4.

The coordinates of the 20 lowest energy models have been deposited in the PDB (accession code: 1GQO); the lowest energy model is the first one in the list.

RESULTS

Structural ensemble

Specific assignment of antiamoebin resonances was achieved using information from various methods including HSQC (Fig. 1), HMBC, COSY and TOCSY. Eighty seven proton-proton distance restraints were derived from nuclear Overhauser-effect spectra (e.g., NOESY, Fig. 2) and subjected to restrained simulated annealing, as described in the Experimental section. Fig. 3 shows the final ensemble of antiamoebin conformers derived from a random starting configuration, superposed about the Cα positions of the lowest energy conformer. Structural statistics for this ensemble are shown in Table 1. The three different superpositions show how alike in structure the conformers of the ensemble are, when aligned about the N- or C-terminal regions separately, and aligned about the entire length of the polypeptide (Fig. 3). This comparison of superpositions suggests that a central, flexible ''hinge'' region, located around residues Gly^7-Aib^9, which may have functional importance, separates the well-defined terminal regions. The root mean square deviations (from the position of the lowest energy conformer) for these alignments are shown in Table 2, and suggest a tightly defined ensemble.

Fig. 4 shows a superposition of the lowest energy conformer of the NMR ensemble and the crystal structure derived from the same solvent (Snook et al., 1998). The structures are aligned about their most closely matched region, residues Aib^9-Iva^{13}. It can be seen that the backbone conformations of the C-termini are very similar, but that toward the N-termini, large differences exist. The crystal structure consists of right-handed helices throughout, whereas the NMR model forms a right-handed helix toward the C-terminal end, but a turn of left-handed helix from residue Leu^8 toward the N-terminus. This is a significant difference in structure, enabled by the achiral amino acids Aib^{3,4,5} and Gly^7, and the D-amino acid Iva^6, which form a contiguous sequence five residues long near the N-terminal end of the polypeptide. This lack of L-form residues is likely to be important in allowing the polypeptide backbone to adopt a left-handed conformation. In none of the simulated annealing runs did we see the anticipated equal distribution of left-handed and right-handed helices, which would arise if the NMR data supported both possibilities. Also, swapping the stereospecific assignments of the resolved pseudoatom terms to specify their stereoisomer(s) still produced model structures with left-handed helices.

Hydrogen bonds in the final ensemble (Table 3) were detected as described in the Experimental section. The most frequently occurring backbone hydrogen bonds were of the (i, $i+3$) type, normally associated with 3_{10}-helices, and are commonly found in peptides containing Aib residues (Toniolo and Benedetti, 1991).

The dependence of the amide chemical shifts on temperature supports the proposed hydrogen bonding character in

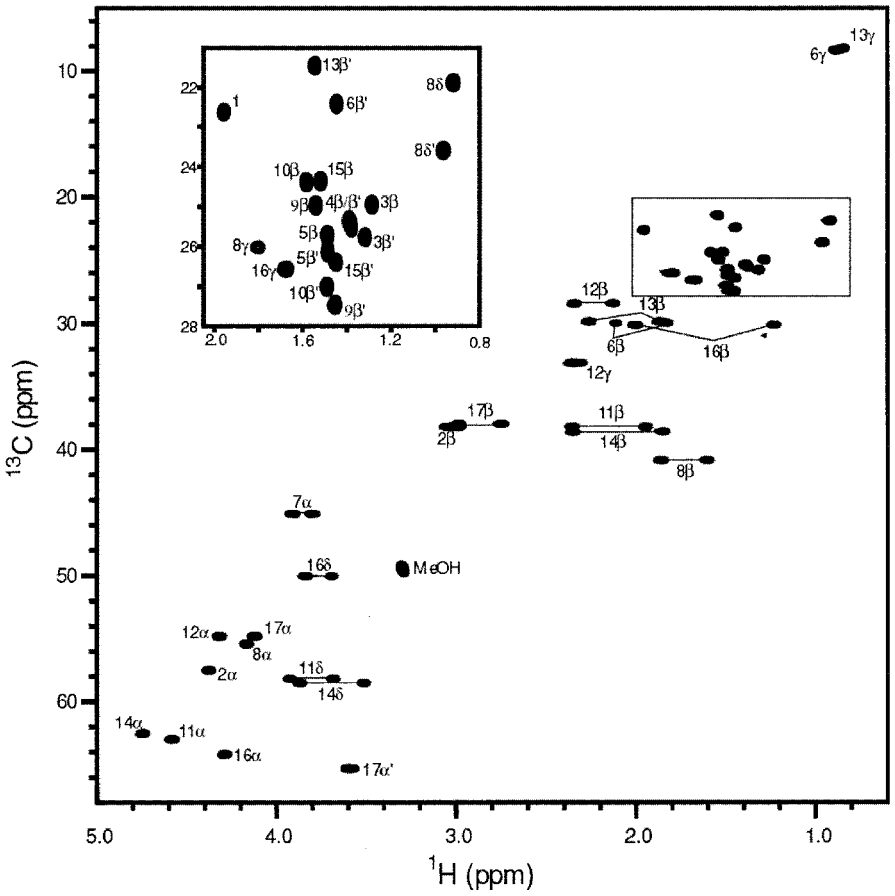

FIGURE 1 ^{13}C-^{1}H-HSQC spectrum showing resonances of protons attached to carbon atoms. Enlargement (*inset*) shows the congested methyl region. Recorded at 298 K.

the model structures produced from the simulated annealing process. The chemical shift temperature dependence results (Fig. 5) suggest that the most strongly hydrogen-bonded amide protons are those on Aib[4], Aib[5], Leu[8], Gln[12], Aib[15], and Phl[17]. From the simulated annealing runs using NOE-derived distance restraints, the amide protons of residues Aib[4], Aib[5], Gly[7], Leu[8], Gln[12], Aib[15], and Phl[17] are all likely to be involved in hydrogen bonding.

Comparing the crystal structure with the NMR data resulted in 16 or 17 violations of the NOE distance restraints of greater than 0.5 Å. The most significant of these violations were those involving residues 4-8, including some resulting from the hydrogen bond restraints (Table 4). Thus it is clear that the NMR and crystal structures are distinct. The remainder of the violations are either between adjacent residues or within a residue, and are likely to be resolved by simple rotation of backbone and side-chain bonds.

DISCUSSION

The peculiarities of the primary structure of antiamoebin have led to a more problematic structure determination than might otherwise be expected for a polypeptide of its size. This can be mainly attributed to the reduced number of spin systems and large numbers of chemically identical groups (due to the primary structure), and the overlapping chemical shifts of these groups, which make NMR data interpretation difficult. A more definitive study would require stereo- and residue-specific isotope labeling, which was beyond the scope of this project on the natural product.

In a previous NMR study of antiamoebin I in dimethylsulphoxide, the results obtained were only sufficient to propose general models for the backbone conformation (Das et al., 1986). That study suggested that the polypeptide was highly ordered in solution, with ten of the backbone amide groups inaccessible to solvent (and therefore likely to be involved in intramolecular hydrogen bonding). The pattern of amide hydrogen bonding proposed by Das et al. was in agreement with that found in this study (Table 3). By analyzing possible hydrogen bonding patterns and specific interresidue NOEs, Das et al. calculated likely backbone angles and concluded that antiamoebin favors a left-handed 3_{10}-helix for residues Aib[3]-Gly[7], with Type II β-turns at the N-terminus and for residues Leu[8]-Aib[9]. The C-terminal segment was proposed to be a 3_{10}-helix, with a right-handed twist being considered more feasible. Our NMR

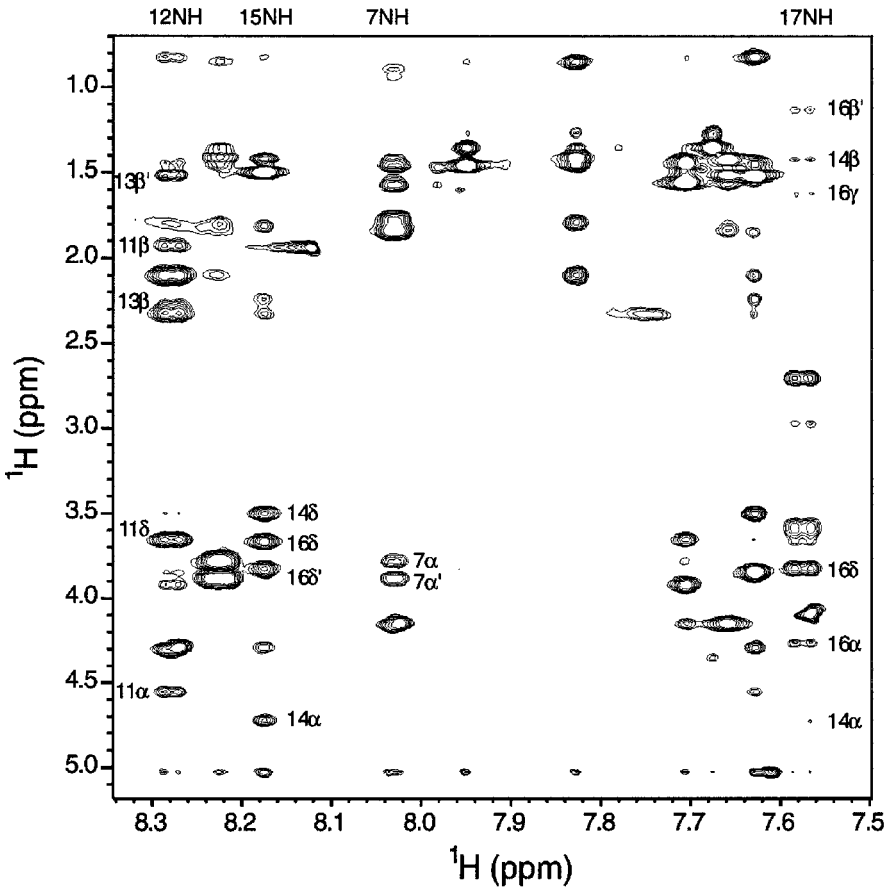

FIGURE 2 Section of a NOESY spectrum showing inter and intraresidue resonance peaks. Recorded at 278 K, 200 ms mixing time.

data has led to a model ensemble that matches these predictions closely.

Detailed NMR and crystal structures exist for other peptaibols, most notably zervamicin (Karle, et al., 1991; Balashova et al., 2000; Shenkarev et al., 2002) and alamethicin (Fox and Richards, 1982; Esposito et al., 1987; Franklin et al., 1994), which form well characterized voltage-gated ion channels. The crystal structures of those peptaibols are broadly similar to that of antiamoebin: they are helical, with a bend near the center caused by an imino acid (Pro or Hyp).

Leu^1-zervamicin is a bent helix, 29 Å long, and has the same number of residues as antiamoebin (16, with an acetylated N-terminus). The central bend is a little less marked than that of antiamoebin, varying between 30° and 45° in the different crystal forms. The crystal structure has an α-helical N-terminal end (from residue 1 to 9), with the C-terminal part being made up of a β-bend ribbon spiral similar to that of antiamoebin (Karle, et al., 1991). The primary structure differs from antiamoebin in that every third or fourth residue is polar, resulting in an amphipathic helix with the polar side chains arranged on one side of the helix. After association of a number of monomers, this allows a hydrophilic ''face'' of the polypeptide to provide solvation to water and ions passing through a central channel, while presenting the more hydrophobic side to the surrounding lipid bilayer. The crystal structures of zervamicin and antiamoebin are close enough for the zervamicin structure to have been used as a search model in the elucidation of the antiamoebin/octanol crystal structure (Karle et al., 1998) and the antiamoebin/methanol structure (Snook et al., 1998; Snook and Wallace, 1999).

Solution structures of zervamicin IIB have been determined by NMR spectroscopy in several isotropic solvents (Balashova et al., 2000). The structures obtained were broadly similar to the crystal structure, with the backbone RMSD between the lowest energy NMR monomer and the crystal structure being ~1.3 Å. Much of this difference can be attributed to slightly different helix bend angles. A recent structure of zervamicin IIB bound to dodecylphosphocholine (DPC) micelles (Shenkarev et al., 2002) found that in the anisotropic environment of the lipid micelle gave rise to a smaller bend angle around Hyp^{10} (23° cf. 47° isotropic solvents), leading to slightly increased length of the peptide in DPC, but otherwise the two NMR structure ensembles were very similar.

Alamethicin has four more residues than zervamicin or antiamoebin, being a 20-mer, and is noticeably longer in

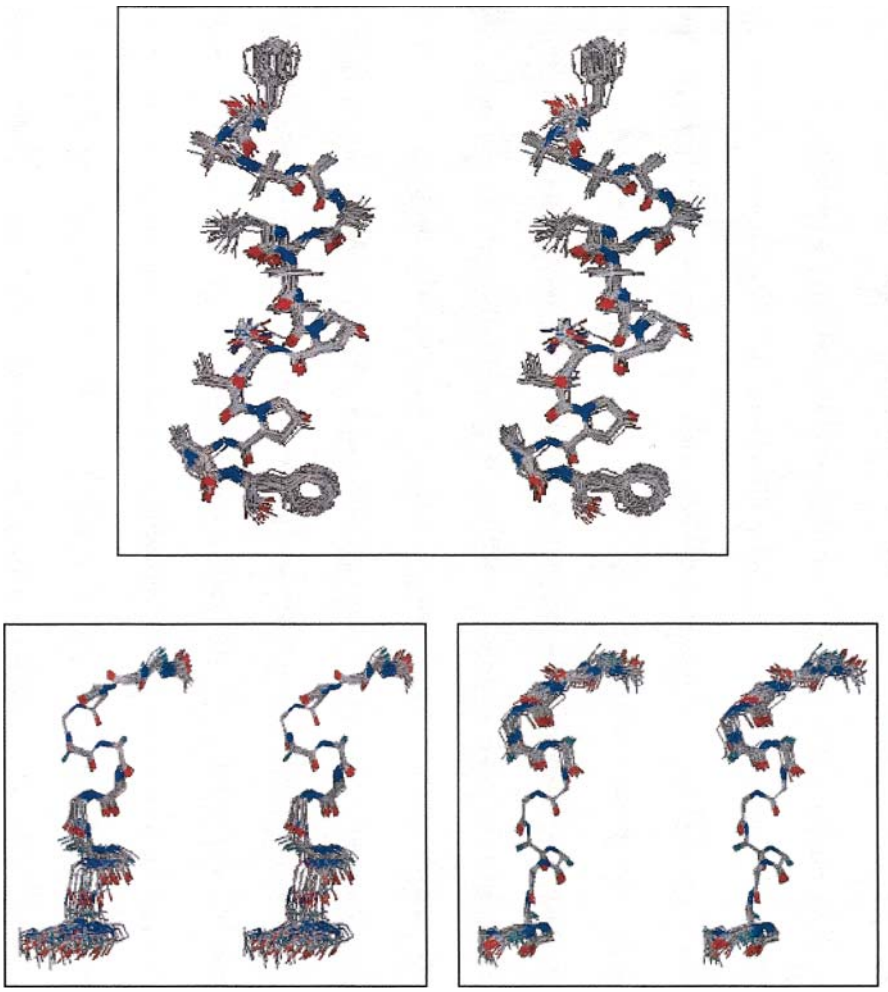

FIGURE 3 Stereo pictures of the 20 lowest energy conformers, aligned about the main chain atoms in all residues (*top*), residues 3-8 (*bottom left*), and residues 9-14 (*bottom right*).

dimension than antiamoebin or zervamicin at around 34 Å. They share common features such as a high proportion of Aib residues, a largely helical structure and the capped termini characteristic of peptaibols. The molecule in the crystal structure (Fox and Richards, 1982) has a less pronounced helix bend angle than antiamoebin or zervamicin, at around 33°, and is mostly α-helical. In SDS micelles, NMR studies found that alamethicin is largely α-helical, with a flexible central segment (Franklin et al., 1994). This flexibility was attributed to the central Pro^{14} residue, and the consequent absence of hydrogen bond partners for the residues in the preceding turn of the helix. However, amide exchange measurements suggest that any disruption in the α-type hydrogen bond network around the Pro^{14} residue is offset by the formation of 3_{10}-type associations when alamethicin is reconstituted in lipid vesicles, (Dempsey and Handcock, 1996) or in methanol solution (Dempsey, 1995), resulting in a stable conformation.

The conformation of antiamoebin in methanol solution, as determined by NMR spectroscopy, differs significantly from the crystal structures previously determined (Snook et al., 1998; Karle et al., 1998).

Violations of the NMR-derived distance restraints and amide hydrogen bonds (Table 4) by the crystal structure show that the crystalline and methanol solution conformations cannot be identical. All the distance restraint violations of greater than 0.5 Å between nonadjacent residues involve those of the most dissimilar region between crystal and NMR structures, residues Aib^4-Leu^8. This is around the region where the NMR models adopt a left-handed helix. All of the

TABLE 1 Structural statistics of the lowest energy ensemble, from X-PLOR (Brünger, 1992) and PROCHECK (Laskowski et al., 1993)

Number of experimental distance restraints	87
Hydrogen bonding distance restraints	7
Average RMSD from all distance restraints (Å)	0.011
Average RMSD from idealized geometry: bonds (Å)	0.013, SD 0.0001
Average RMSD from idealized geometry: angles (°)	2.92, SD 0.017
Average RMSD from idealized geometry: impropers (°)	6.62, SD 0.028
Residues in favored regions (%)	25.0
Residues in allowed regions (%)	33.3
Residues in generously allowed regions (%)	41.7
Residues in disallowed regions (%)	0.0

TABLE 2 RMS deviations from the position of the lowest energy conformer for the ensemble, aligned about the Cα atoms of three different residue ranges

Alignment	Mean backbone RMSD for aligned residues (Å)	Mean backbone RMSD for whole ensemble (Å)
N-term: Aib^{3}-Leu^{8}	0.33	2.8
C-term: Aib^{9}-Hyp^{14}	0.60	3.4
All: Ace^{1}-Phl^{17}	1.73	1.7

violations are of the same type: the specified atoms are too far apart to satisfy the NMR data, due to the opposite-handed twist of the helix. This effect can be clearly seen (Fig. 4), where the backbone worms tracing the Cα backbone atoms are nearly mirror images of one another. The amide protons of residues Aib^{4} and Aib^{5} are likely to be involved in hydrogen bonding, as shown by the temperature dependence results (Fig. 5) and identification using the HBPLUS and SYBYL programs (Table 3). Because these amides were not found to be hydrogen bonded in the crystal structure, this represents a significant difference in structure between the two forms.

The NMR models have a fairly similar conformation to the crystal structure in the C-terminal half of the polypeptide, that of a right-handed 3_{10}-helix. However, a putative ''hinge'' region is observed in the center of the molecule (which may be functionally important), and the residues toward the N-terminus adopt a left-handed 3_{10}-helix conformation. One reason that antiamoebin in solution but not in the solid state could adopt this unusual conformation is the lack of crystal packing forces, which constrain the polypeptide in crystals. This is essentially the only major difference between the two systems, both having been studied in the same solvent and at similar temperatures.

The ''hinge'' region in the center of the NMR models may have functional importance for the insertion of the peptide into lipid membranes. The methods of insertion proposed for alamethicin (Boheim, 1974; Fox and Richards, 1982; Cascio and Wallace, 1988; He et al., 1996; Tieleman et al., 2001), suggest that the orientation of the peptide and its response to a transmembrane voltage is affected by the helix dipole of the polypeptide. In the absence of charged amino acids (as is the case in uncharged alamethicin variants, and in antiamoebin) this effect may be even more important, as the dipole is the only source of electrostatic interaction with the transmembrane potential (Dempsey and Handcock, 1996). It would seem plausible that flexibility in the center of the peptide would make this insertion more favorable, though the molecular dynamics studies for the recently proposed mechanism for alamethicin insertion (Tieleman et al., 2001) did not show significant change in the helix bend angle.

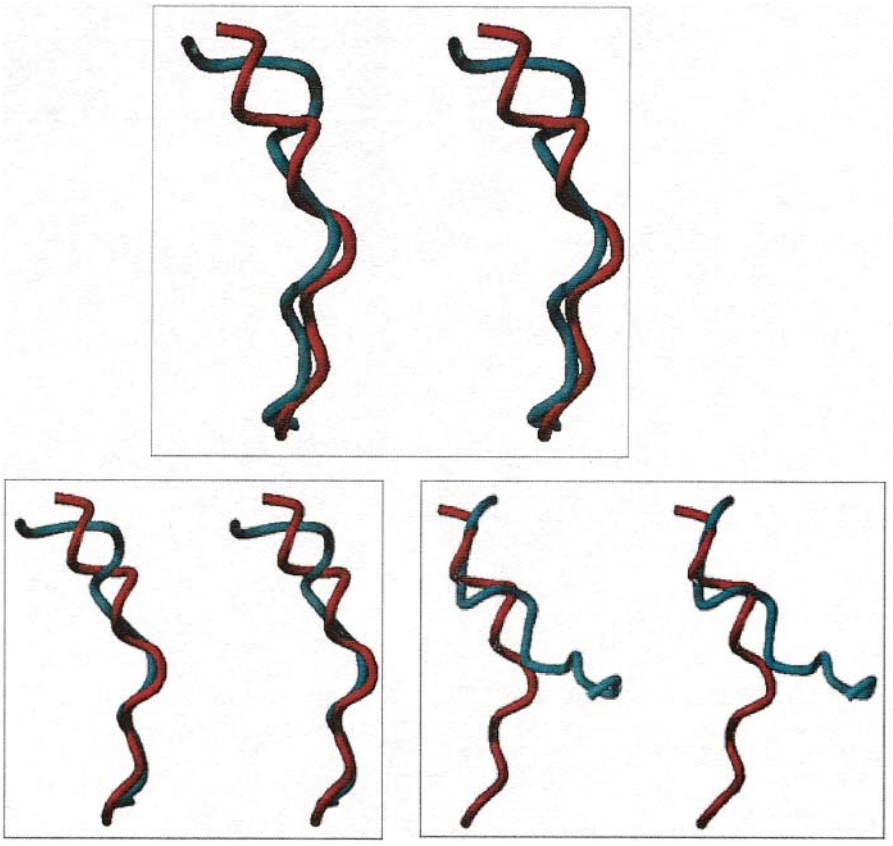

FIGURE 4 Stereo views of the lowest energy NMR conformer (*cyan*) aligned with the crystal structure (*red*: Snook et al., 1998) about the Cα atoms of residues 1-17 (*top*), residues 3-8 (*bottom left*), and residues 9-14 (*bottom right*).

TABLE 3 Hydrogen bond associations for antiamoebin, in the crystal structure (Snook et al., 1998) and the lowest energy NMR ensemble (in the latter the percentage of NMR conformers detected that have the hydrogen bond is noted in parentheses)

	Crystal structure	NMR (% of final ensemble)
Donor NH	Acceptor O	Acceptor O
Aib 4	–	Phe 2 (100)
Aib 5	–	Phe 2 (100)
Iva 6	Phe 2	–
Gly 7	Aib 3	Aib 4 (100)
Leu 8	Aib 4	Aib 4 (15)
Leu 8	–	Aib 5 (100)
Aib 9	Aib 5	Aib 5 (25)
Aib 10	Iva 6	Gly 7 (100)
Gln 12	Aib 9	Aib 9 (100)
Iva 13	Aib 10	–
Aib 15	Gln 12	Iva 13 (100)
Phl 17	Hyp 14	Hyp 14 (20)

One question that arises for all of the studies of peptaibols in organic solvents is the relevance of the structures determined in these environments to their structures in membranes. Circular dichroism spectroscopy has been used to demonstrate the membrane-mimetic nature of these solvents for a number of these channel-forming molecules (Cascio and Wallace, 1988; Duclohier and Wroblewski, 2001). In the case of antiamoebin, the CD spectra in membranes and in methanol solution (Snook et al., 1998) are very similar but not identical, which suggests some conformational change may occur upon membrane insertion.

A mechanism for the membrane insertion of antiamoebin is proposed (Fig. 6), based on the findings in this study and consideration of other peptaibol insertion models discussed above. Before binding of the target membrane, antiamoebin is likely to exist as a monomer. The conformational freedom allowed by being in solution suggests that the NMR-derived structures (Fig. 3) may be relevant. Upon association with the membrane, the polypeptide may become more helical, as is observed with alamethicin. Channel formation of antiamoebin appears to be a less voltage-dependent, but more lipid-specific process (Duclohier et al., 1998) than found for alamethicin, and is likely to involve either a partial refolding or the reorientation of the molecular dipole with respect to the bilayer normal (Snook et al., 1998). The ordered nature of the bilayer, like that in the crystal, may induce conformational change during insertion of the peptide, and the anisotropy of the lipid could promote a straightening of the bend in antiamoebin. It is assumed that antiamoebin inserts as a monomer, and that monomers subsequently associate to form the conducting pore. Conductance studies by Duclohier et al. (1998) suggest that the antiamoebin channel will contain $4n$ monomers, and models for an octameric channel model which has an appropriate size to fit with these measurements have been proposed (Wallace et al., 2000). The insertion is likely to occur in a manner generally similar to the accepted ''barrel-stave'' model for alamethicin (reviewed by Sansom, 1993), which has also been suggested to be the mode of pore formation for zervamicin IIB (Shenkarev et al., 2002). However, the differences in channel-formation properties between antiamoebin and these other peptaibols (Snook et al., 1998; Duclohier et al., 1998) indicate there are subtle differences in the mechanisms, and are consistent with the more drastic structural rearrangement proposed for antiamoebin in this model.

In summary, the NMR structures presented in this study suggest that antiamoebin is more sensitive to environmental factors than was previously thought (Snook et al., 1998; Wallace et al., 2000). Although the NMR models may not represent the active structure of antiamoebin in membranes, they nonetheless provide insight into the flexibility and

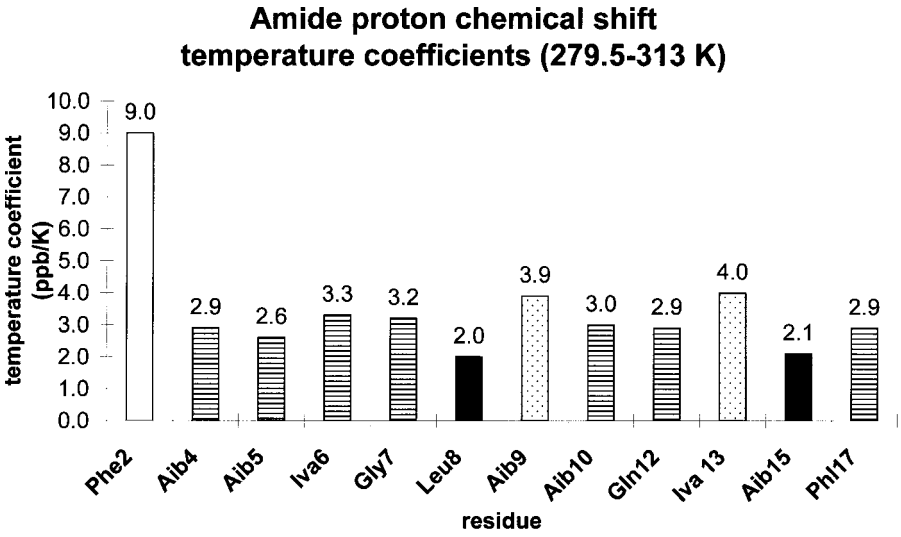

FIGURE 5 Bar chart showing temperature coefficients for antiamoebin amide proton chemical shifts, designated by their likelihood of being involved in hydrogen bonding. Black (<2.5 ppb/K) signifies very likely; horizontal stripe (2.5–3.5 ppb/K) signifies likely; dots (3.5–4.0 ppb/K) signifies unlikely; white (>4.0 ppb/K) signifies very unlikely.

TABLE 4 NOE distance restraint violations (>±0.5 Å) between nonadjacent residues, and inconsistent amide proton chemical shift temperature dependence, from the crystal structure (Snook et al., 1998)

Restraint atoms	Restraint distance range (Å)	Measured distance, crystal chain A (Å)	Measured distance, crystal chain B (Å)
Aib^4 HN–Phe^2 Hβ^1	3.2–4.0	4.8	6.0
Aib^5 HN–Phe^2 Hβ^1	3.0–4.6	5.6	No violation
Leu^8 HA–Aib^4 HN	3.0–4.6	8.6	8.7
Leu^8 Hβ^1–Aib^5 HN	2.8–4.4	7.2	7.2
Aib^4 HN hydrogen bond	1.5–2.3	No hydrogen bond	No hydrogen bond
Aib^5 HN hydrogen bond	1.5–2.3	No hydrogen bond	No hydrogen bond

adaptability of channel-forming polypeptides, and may represent one of many intermediates in the process of membrane insertion.

This study was supported by the Biotechnology and Biological Sciences Research Council (with a studentship for T.P.G. and funding for the Bloomsbury Centre for Structural Biology).

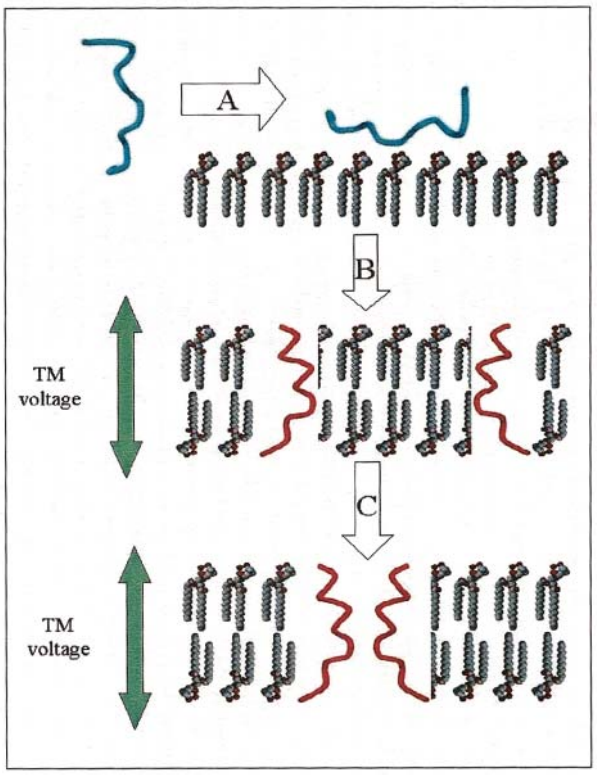

FIGURE 6 Schematic diagram showing a possible insertion model for antiamoebin in a lipid bilayer (shown in *cross section*). (*A*) Monomeric antiamoebin binds to the target membrane. (*B*) On application of a transmembrane voltage, antiamoebin inserts into the membrane. (*C*) Antiamoebin monomers assemble to form the active channel. The polypeptide structures shown are Cα backbone worms representing the lowest energy NMR model (*cyan*: this work) and the crystal structure (*red*: Snook et al., 1998).

REFERENCES

Anders, R., O. Ohlenschlager, V. Soskic, H. Wenschuh, B. Heise, and L. R. Brown. 2000. The NMR solution structure of the ion channel peptaibol chrysospermin C bound to dedecylphosphocholine micelles. *Eur. J. Biochem.* 267:1784–1794.

Bailey, S. 1994. The CCP4 Suite - programs for protein crystallography. *Acta Crystallogr. D.* 50:760–763.

Balashova, T. A., Z. O. Shenkarev, A. A. Tagaev, T. V. Ovchinnikova, J. Raap, and A. S. Arseniev. 2000. NMR structure of the channel-former zervamicin IIB in isotropic solvents. *FEBS Lett.* 466:333–336.

Boheim, G. 1974. Statistical analysis of alamethicin channels in black lipid membranes. *J. Membr. Biol.* 19:277–303.

Borgias, B. A., and T. L. James. 1989. Two-dimensional nuclear Overhauser effect - complete relaxation matrix analysis. *Methods Enzymol.* 176:169–183.

Borgias, B. A., and T. L. James. 1990. MARDIGRAS - A procedure for matrix analysis of relaxation for discerning geometry of an aqueous structure. *J. Mag. Res.* 87:475–487.

Brünger, A. T. 1992. X-PLOR v3.1. A System for X-ray Crystallography and NMR. Yale University Press, New Haven.

Cascio, M., and B. A. Wallace. 1988. Conformation of alamethicin in phospholipid vesicles: implications for insertion models. *Proteins.* 4:89–98.

Chugh, J., and B. A. Wallace. 2001. Peptaibols: Models for ion channels. *Biochem. Soc. Trans.* 29:565–570.

Das, M. K., S. Raghothama, and P. Balaram. 1986. Membrane channel forming polypeptides - molecular-conformation and mitochondrial uncoupling activity of antiamebin, an alpha-aminoisobutyric-acid containing peptide. *Biochemistry.* 25:7110–7117.

Dempsey, C. E. 1995. Hydrogen-bond stabilities in the alamethicin helix – pH-dependent amide exchange measurements in methanol. *J. Am. Chem. Soc.* 117:7526–7534.

Dempsey, C. E., and L. J. Handcock. 1996. Hydrogen bond stabilities in membrane-reconstituted alamethicin from amide-resolved hydrogen-exchange measurements. *Biophys. J.* 70:1777–1788.

Di Blasio, B., V. Pavone, M. Saviano, A. Lombardi, F. Nastri, C. Pedone, E. Benedetti, M. Crisma, M. Anzolin, and C. Toniolo. 1992. Structural characterization of the beta-bend ribbon spiral - crystallographic analysis of 2 long (L-Pro-Aib_n) sequential peptides. *J. Am. Chem. Soc.* 114:6273–6278.

Duclohier, H., and H. Wroblewski. 2001. Voltage-dependent pore formation and antimicrobial activity by alamethicin and analogues. *J. Membr. Biol.* 184:1–12.

Duclohier, H., C. F. Snook, and B. A. Wallace. 1998. Antiamoebin can function as a carrier or as a pore-forming peptaibol. *Biochim. Biophys. Acta.* 1415:255–260.

Esposito, G., J. A. Carver, J. Boyd, and I. D. Campbell. 1987. High resolution ^{1}H NMR study of the solution structure of alamethicin. *Biochemistry.* 26:1043–1050.

Fox, R. J., and F. M. Richards. 1982. A voltage gated ion channel model inferred from the crystal structure of alamethicin at 1.5Å resolution. *Nature.* 300:325–330.

Franklin, J. C., J. F. Ellena, S. Jayasinghe, L. P. Kelsh, and D. S. Cafiso. 1994. Structure of micelle-associated alamethicin from ^{1}H NMR - evidence for conformational heterogeneity in a voltage-gated peptide. *Biochemistry.* 33:4036–4045.

Gratias, R., R. Konat, H. Kessler, M. Crisma, G. Valle, A. Polese, F. Formaggio, C. Toniolo, Q. B. Broxterman, and J. Kamphuis. 1998. First step toward the quantitative identification of peptide 3_{10}-helix conformation with NMR spectroscopy: NMR and X-ray diffraction structural analysis of a fully-developed 3_{10}-helical peptide standard. *J. Am. Chem. Soc.* 120:4763–4770.

He, K., S. J. Ludtke, W. T. Heller, and H. W. Huang. 1996. Mechanism of alamethicin insertion into lipid bilayers. *Biophys. J.* 71:2669–2679.

Hoogstraten, C. G., and J. L. Markley. 1996. Effects of experimentally achievable improvements in the quality of NMR distance constraints on the accuracy of calculated protein structures. *J. Mol. Biol.* 258:334–348.

Jaworski, A., and H. Brukner. 2000. New sequences and new fungal producers of peptaibol antibiotics antiamoebin. *J. Pept. Sci.* 6:149–167.

Karle, I. L., M. A. Perozzo, V. K. Mishra, and P. Balaram. 1998. Crystal structure of the channel-forming polypeptide antiamoebin in a membrane-mimetic environment. *Proc. Natl. Acad. Sci. USA.* 95:5501–5504.

Karle, I. L., J. L. Flippen-Anderson, S. Agarwalla, and O. Balaram. 1991. Crystal-structure of [Leu^1]zervamicin, a membrane ion-channel peptide - implications for gating mechanisms. *Proc. Natl. Acad. Sci. USA.* 88:5307–5311.

Laskowski, R. A., M. W. MacArthur, D. S. Moss, and J. M. Thornton. 1993. PROCHECK - a program to check the stereochemical quality of protein structures. *J. Appl. Crystallogr.* 26:283–291.

Marion, D., M. Ikura, R. Tschudin, and A. Bax. 1989. Rapid recording of 2D NMR-spectra without phase cycling - application to the study of hydrogen-exchange in proteins. *J. Mag. Res.* 85:393–399.

McDonald, I. K., and J. M. Thornton. 1994. Satisfying hydrogen-bonding potential in proteins. *J. Mol. Biol.* 238:777–793.

Pandey, R. C., H. Meng, J. C. Cook, and K. L. Rinehart. 1977. Structure of antiamoebin I from high resolution field desorption and gas chromatographic mass spectrometry studies. *J. Am. Chem. Soc.* 99:5203–5205.

Pandey, R. C., H. Meng, J. C. Cook, and K. L. Rinehart. 1978. Structure of the peptide antibiotic antiamoebin II. *J. Antibiot.* 31:241–243.

Sansom, M. S. P. 1993. Structure and function of channel-forming peptaibols. *Q. Rev. Biophys.* 26:365–421.

Shenkarev, Z. O., T. A. Balashova, R. G. Efremov, Z. A. Yakimenko, T. V. Ovchinnikova, J. Raap, and A. S. Arseniev. 2002. Spatial structure of zervamicin IIB bound to DPC micelles: implications for voltage-gating. *Biophys. J.* 82:762–771.

Sklenar, V., M. Piotto, R. Leppik, and V. Saudek. 1993. Gradient-tailored water suppression for ^{1}H-^{15}N-HSQC experiments optimized to retain full sensitivity. *J. Mag. Res. Series A.* 102:241–245.

Snook, C. F., and B. A. Wallace. 1999. The molecular-replacement solution of an intermediate-sized helical polypeptide, antiamoebin I. *Acta Crystallogr. D*55:1539–1545.

Snook, C. F., G. A. Woolley, G. Oliva, V. Pattabhi, S. P. Wood, T. L. Blundell, and B. A. Wallace. 1998. The structure and function of antiamoebin I, a proline-rich membrane-active polypeptide. *Structure.* 6:783–792.

Tieleman, D. P., H. J. C. Berendsen, and M. S. P. Sansom. 2001. Voltage-dependent insertion of alamethicin at phospholipid/water and octane/water interfaces. *Biophys. J.* 80:331–346.

Thirumalachur, M. J. 1968. Antiamoebin, a new antiprotozoal-antihelmintic antibiotic. Part 1. Production and biological studies. *Hindustan Antibiot. Bull.* 10:287–289.

Toniolo, C., and E. Benedetti. 1991. The polypeptide 3_{10} helix. *TIBS.* 16:350–353.

Toniolo, C., E. Peggion, M. Crisma, F. Formaggio, X. Q. Shui, and D. S. E. Eggleston. 1994. Structure determination of racemic trichogin A IV using centrosymmetric crystals. *Nat. Struct. Biol.* 1:908–914.

Vanopdenbosch, N., R. Cramer, and F. F. Giarrusso. 1985. SYBYL, the integrated molecular modeling system. *J. Mol. Graph.* 3:110–111.

Wallace, B. A. 2000. Common structural features in gramicidin and other ion channels. *Bioessays.* 22:227–234.

Wallace, B. A., C. F. Snook, H. Duclohier, and A. O. O'Reilly. 2000. Antiamoebin: A polypeptide ion carrier and channel. *In* Peptides for the New Millennium. G. B. Fields, J. P. Tam, and G. Barany, editors. Kluwer Academic Publishers, Dordrecht. 733–735.

Wüthrich, K. 1986. NMR of Proteins and Nucleic Acids. John Wiley, New York.